International Journal of Physical Sciences Vol. 7(14), pp. 2174 - 2180, 30 March, 2012
Available online at http://www.academicjournals.org/IJPS
DOI: 10.5897/IJPS11.1543
ISSN 1992 - 1950 ©2012 Academic Journals

Full Length Research Paper

First-principles study on La-doped ZnO used as transparent electrode for optoelectronic device

Wei Peng, Yun Zeng*, Cheng-Bin Zhang, Yong-Hong Yan and Wei Hu

School of Physics and Microelectronics Science, Hunan University, Changsha 410082, Peoples Republic of China.

Accepted 19 March, 2012

A systematic study on electronic and optical properties of wurtzite zinc oxide (ZnO) with different La-doping concentrations has been performed. The calculations are based on the first principles plane-wave pseudopotential method with the density functional theory (DFT) and the generalized gradient approximation (GGA). According to the results, the band gap of ZnO is broadened due to the increase of La-doping concentrations. By La-doping, the decrease of absorption coefficient and the blueshift of absorption edge are obtained. In addition, there is a strong interaction between the La atom and the surrounding atoms, because the high electron density overlaps. By Mulliken population analysis, we found out that the metallization effect appears due to the increase of La-doping concentration, which demonstrates that the La-doped ZnO is a potential material as a low absorption coefficient semiconductor material. The simulation and calculation results are in good agreement with the existing experimental data and the study can provide a theoretical basis for future applications of La-doped ZnO as a semi-transparent electrode.

Key words: Zinc oxide (ZnO), La, first-principles, transparent electrode, electronic properties, optical properties.

INTRODUCTION

Zinc oxide (ZnO) is an important semiconductor compound of the II-VI group with a wide direct band-gap of 3.37 eV at 300K and a large exciton binding energy of 60 meV (Li et al., 2010; Ramakrishna et al., 2000). It is a potential candidate material for ultraviolet and blue light-emitting diodes and electro-luminescent displays (Anandan et al., 2007). It has also attracted considerable attention in recent years owing to its photocatalytic ability in the degradation of various environmental pollutants, such as pesticides, detergents, dyes and volatile organic compounds into carbon dioxide, water and mineral acids under ultraviolet (UV) light irradiation (Hoffmann et al., 1995; Sehili et al., 1989). Moreover, ZnO is believed to be one of the most promising materials for the detection, the windows layers of solar cells and the surface acoustic wave devices (Chowdhury et al., 2010).

During the past decades, doped with an optically active luminescence center, ZnO nanocrystallites create new opportunities for luminescent study and application of nanometer scale material (Sans et al., 2005; Tang et al., 2008). Doped with transition-metal element or rare-earth element, ZnO can be used as effective phosphor materials (Kim and Seshadri, 2008; Yu et al., 2009). It has already been reported that La-doped ZnO film (ZnO:La) exhibits excellent violet and green light-emitting properties, and the band gap can be modulated by varying the doping concentrations. Lan et al. (2007) studied the structural and optical properties of ZnO:La films prepared on quartz substrates by RF magnetron sputtering. With the increase of doping level, the band gap of ZnO films evaluated by the linear fitting linearly increase from 3.270 to 3.326 eV. The average transmittance in the visible range is over 80%, and a blueshift of the absorption edge is observed (Lan et al., 2007). Unfortunately, the principles of the variation of

*Corresponding author. E-mail: yunzeng@hnu.edu.cn, huwei@hnu.edu.cn.

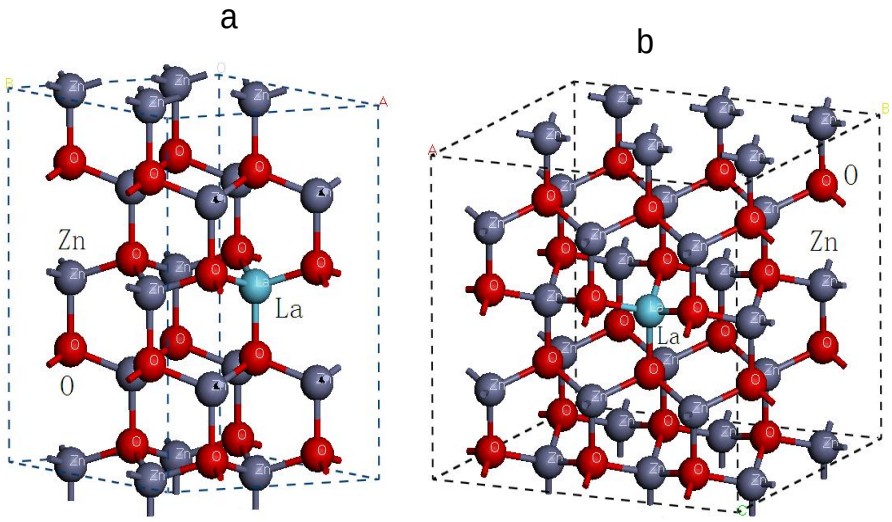

Figure 1. ZnO supercells for calculation (a) Model 3 with 2×2×2 supercell and (b) Model2 with 3×2×2 supercell. One of the Zn atoms was substituted by one La atom in each supercell.

Table 1. Models of ZnO:La supercell.

Model	Supercell range	Atoms number	Concentration of doped La (%)
M1($Zn_{16}O_{16}$)	2×2×2	32 (Zn:16, O:16)	0
M2($Zn_{23}LaO_{24}$)	3×2×2	48 (Zn:23, O:24, La:1)	4.17
M3($Zn_{15}LaO_{16}$)	2×2×2	32 (Zn:15, O:16, La:1)	6.25

band gap and optical properties have not been systematically studied. Moreover, whether the metallization takes place in La-doped ZnO system has not been discussed.

In this paper, we study the electronic and optical properties of ZnO:La using first-principles calculations based on density functional theory (DFT) and generalized gradient approximation (GGA) in Material Studio 4.0. Our results show that the existence of doped La atoms leads to wider energy gap due to the contribution of La-5d valence electrons and the absorption threshold of ZnO:La systems is considerably blueshifted. Subsequently, the atomic populations (Mulliken) and difference of the charge density contour of the ZnO supercells with different La-doping concentration are also studied. In the end, comparison between calculation results and experimental data is also performed.

COMPUTATIONAL APPROACH

The ideal ZnO has a hexagonal wurtzite structure with the space group P63/mc and C6v-4 symmetry, with two Zn atoms and two O atoms in each primitive cell. The cell parameters are a=b=0.32493 nm, c=0.52054 nm, $\alpha=\beta=90°$ and $\gamma=120°$ (Vispute et al., 1998). Based on the primitive cell, a series of ZnO supercells with and without La-doping were constructed and calculated to investigate the effect of La on the properties of ZnO, as shown in Figure 1 and Table 1.

Numerical calculations were carried out by CASTEP in material studio 4.0 based on first principles. The GGA with the Perdew Burke Ernzerhof exchange-correlation functional were employed in the simulations. Ultrasoft pseudopotential was used to describe the electron-ion interaction. The energy cutoff (Ecut) of plane wave functions was set at 380.0 eV, which was confirmed to be large enough. All atomic positions in the ZnO supercell had been relaxed according to the total energy and force using the Broyden Fletcher Goldfarb Shanno (BFGS) scheme, based on the cell optimization criterion (RMS force of 0.01 eV/Å, stress of 0.02 GPa and displacement of 5.0×10-4 Å). The calculation of total energy and electronic was followed by cell optimization with Survey of Consumer Finance (SCF) tolerance of 5.0×10-6 eV/atom (Xie et al., 2010).

RESULTS AND DISCUSSION

Structural optimization

The optimization of the supercell is the first step in the calculation. We performed a series of calculations for cell optimization and the optimized result of the supercell of pure ZnO is a=b=0.32845 nm, c=0.52939 nm, which is a good agreement with the experimental results

Table 2. Lattice parameters at the different concentration of La.

Model	Concentration of doped La (%)	Lattice parameter (nm)	c/a
M1($Zn_{16}O_{16}$)	0	a=0.32845,c=0.52939	1.6118
M2($Zn_{23}LaO_{24}$)	4.17	a=0.33220,c=0.53452	1.6090
M3($Zn_{15}LaO_{16}$)	6.25	a=0.33478,c=0.53669	1.6031

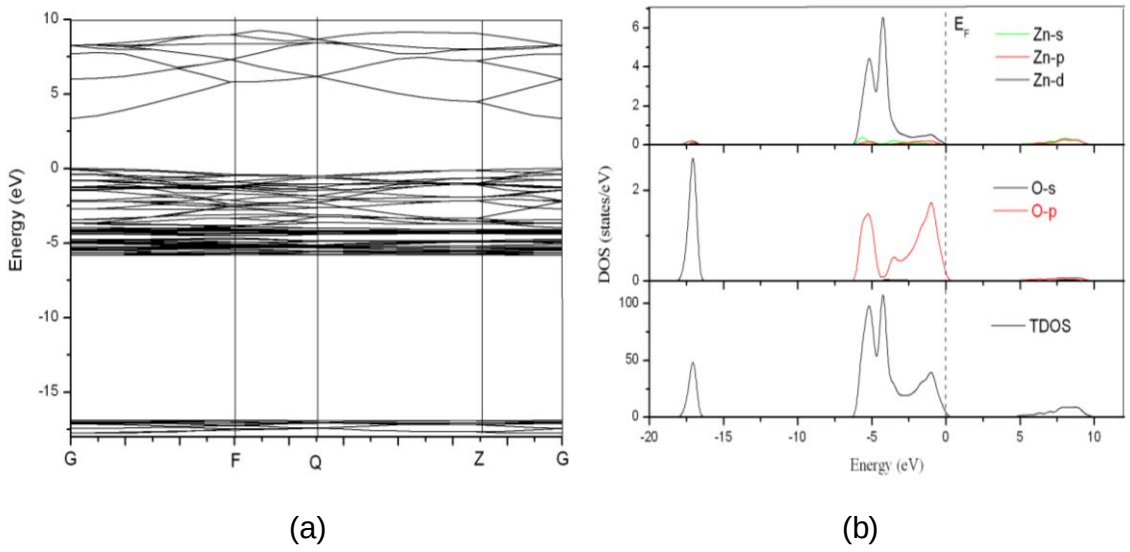

Figure 2. Energy band structure (a) and DOS (b) of pure ZnO supercell.

(a=b=0.32501 nm, c=0.52071 nm) (Kisi and Elcombe, 1989). Thus, the same calculation condition was adopted to calculate the geometrical, electronic and energetic structures of the ZnO with and without La-doping. The optimized results of the ZnO:La supercells are presented in Table 2. Due to the longer bond length of La-O than that of Zn-O, the lattice parameters increased with the concentration of La as shown in Table 2.

Electronic structure

Figure 2 illustrates the calculated band structures (BS), partial and total electronic density of states (PDOS and TDOS) of pure ZnO supercell system. The Fermi-level has been specified to be zero in this paper. It can be seen that the bottom of the conduction band and top of the valence band are at the same k-point (G), which is the representative characteristic for direct gap semi-conductors. In local density functional theory, neglecting of excitation state during Kohn-Sham function's calculation results in lower energy levels above valence band in calculation energy band than that of experimental results, while, the energy levels below valence band in calculation are consistent with the experimental results. Thus, the energy gap in the first principles calculation, based on local density functional theory is lower than that in the experiment. The calculated band gap of pure ZnO in this paper is 0.743 eV, which is in good agreement with other calculations, but obviously lower than experimental one (3.37 eV). Therefore, scissors approximation with the value of 2.627 eV will be adopted in the calculation (Lyons et al., 2009; Xie et al., 2011).

Figure 2 shows the TDOS of ZnO and the PDOS of Zn and O atoms. It should be noted that a sharp TDOS peak of ZnO appears at about -17 eV, which is mainly from O-s state. The valence band above -6.2 eV of ZnO can be divided into two regions: the lower part from -6.2 to -4.3eV and the upper part from -4.3 to about 0 eV, of which the lower valence band is contributed by a mixture of 3d states of Zn and 2p states of O, while the upper part comes mainly from 2p states of O. The conduction band of ZnO is mainly composed of the 4s state of Zn and 2p state of O. A significant charge transfer from Zn (4s) to O (2p) orbits is as shown in Table 3 and a overlap between the Zn (4s) and O (2p) valence electrons as shown in Figure 2 reveals ionic bond between the first nearest neighbor (FNN) Zn-O in pure ZnO.

The energy band structures and DOS in $3\times2\times2$ (M2) and $2\times2\times2$ (M3) ZnO:La supercell are, respectively depicted in Figures 3 and 4. Compared to the pure ZnO supercell model, the doped La atoms lead to a notable

Table 3. Atomic populations (Mulliken) of the ZnO supercells.

Specie	M1($Zn_{16}O_{16}$)		M2($Zn_{23}LaO_{24}$)			M3($Zn_{15}LaO_{16}$)		
	Zn	O	Zn	O	La	Zn	O	La
s	0.49	1.86	0.59	1.86	1.91	0.55	1.86	1.87
p	0.72	4.96	0.72	4.95	6.02	0.73	4.95	6.11
d	9.97	0	9.98	0	1.39	9.98	0	1.42
Total	11.18	6.82	11.28	6.81	9.32	11.25	6.81	9.39
Charge (e)	0.82	-0.82	0.72	-0.80	1.68	0.75	-0.81	1.61

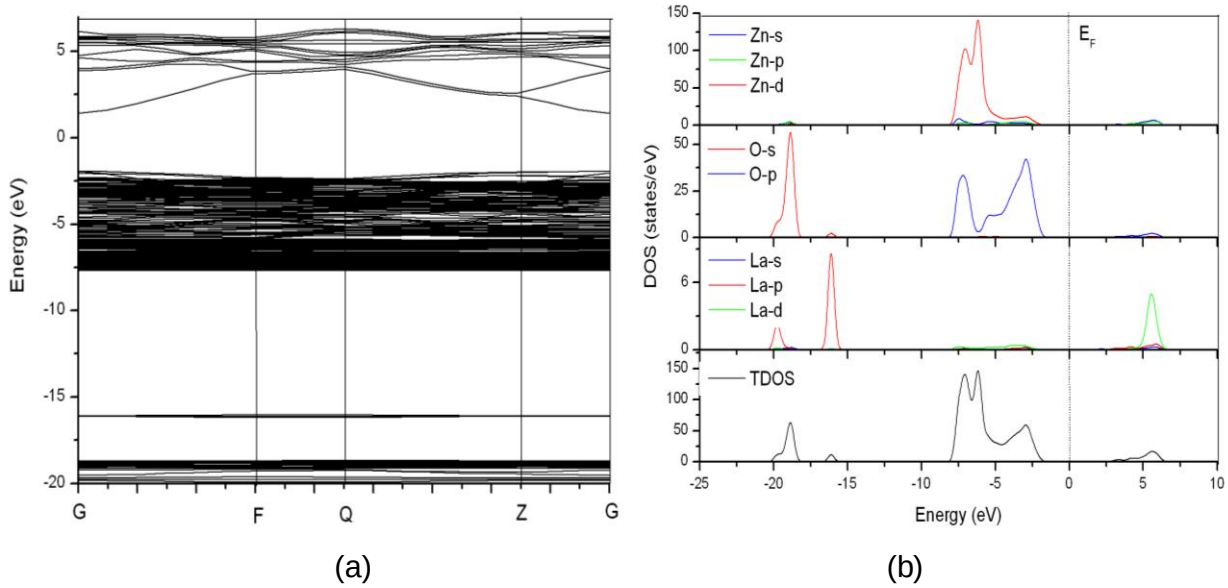

Figure 3. Energy band structure (a) and DOS (b) of 3×2×2 (M2) ZnO:La supercell.

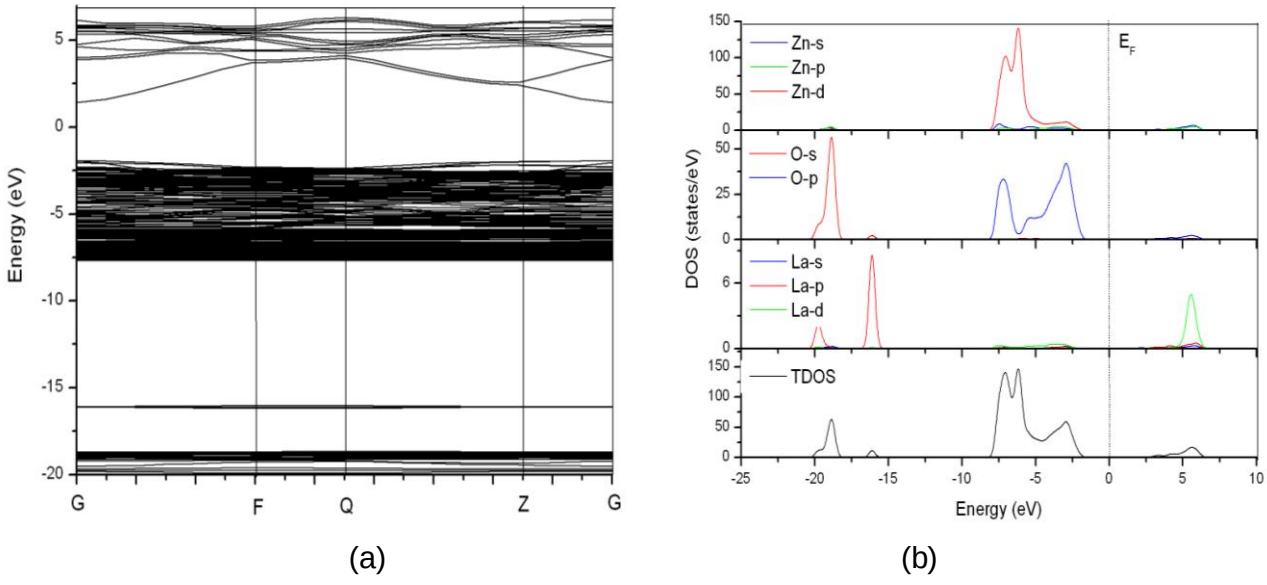

Figure 4. Energy band structure (a) and DOS (b) of 2×2×2 (M3) ZnO:La supercell.

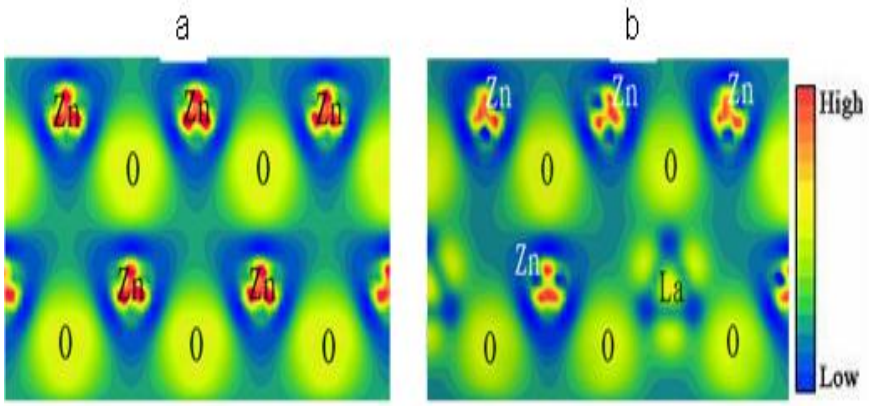

Figure 5. Plots (001) surface of difference of the charge density contour for ZnO supercells with and without La-doping. (a) M1 and (b) M3.

variation of the energy band structure in the La doped ZnO system. For La doped ZnO systems, a large number of surplus electrons exist in the bottom of the conduction band and the states of electrons have degenerated. The bottom of conduction band and the top of valence band both move toward the lower energy level. However, variation extent of the former is much smaller than the latter one. Therefore, energy gap in ZnO system with La-doping increases comparing to the pure ZnO system, such as 3.38 and 3.48 eV for the M2 and M3 models, respectively, as shown in Figures 3 and 4. The band gap in ZnO system broadened with the increasing La-doping concentration, which is verified by the experiment (Lan et al., 2007).

Total DOS is separated to three regions in higher concentration La-doping ZnO system (M3), that is, higher energy region (2.5 to 6 eV), lower energy region (-8.3 to -2.3 eV) and the energy region below -16 eV, as shown in Figure 4. For the higher energy region, the bonding electrons mainly come from the valence electrons of La (d) orbits. The bonding electrons in the lower energy region are mainly contributed by the valence electrons of Zn (d) and O (p) orbits, while the bonding electrons below -16 eV mainly originate from the contribution of valence electrons of La (p) and O (s) orbits. An overlap between La (p) and O (s) orbits reveals that the La (p) to O (s) hybridization has emerged and chemical bonds have been formed in this region.

As discussed earlier, the bonding electrons in higher energy region mainly come from the valence electrons of La (d) orbits. In addition, only weak metallic bonding between the FNN La-Zn is observed in La doped ZnO systems. Thus, more bonding electrons near the Fermi energy level in higher concentration La doped ZnO supercell (M3) are achieved when compared with M2, as shown in Figure 3. As shown in Table 3, one La atom losses 1.68 and 1.61 electrons, and its FNN one Zn atom losses 0.72 and 0.75 electrons, while, one O atom nearby La atom accepts 0.8 and 0.81 electrons, respectively, in La-doped ZnO supercell models M2 and M3. The results show that more than one free electron exists in La-doped ZnO supercells, and it may result in metallization of the La-doped ZnO systems (Wan et al., 2008; Pauporte and Lincot, 1999).

In order to further study the influence induced by La-doping on electronic interaction, the plots of difference of charge density contour on the (001) and (110) plane of the ZnO supercell with and without La-doping are as shown in Figures 5 and 6. As shown in Figures 5 and 6, the distribution of electrons is of great difference in the undoped and doped circumstances. For the pure ZnO system, the directional characteristics of electronic cloud were conspicuous. Thus, the combine force between Zn and O atoms mainly comes from the covalent bond, and only weak ionic bond is found in pure ZnO system. After doping La into ZnO, the ionic bond becomes stronger, covalent bond weaker and the charge cloud is more inhomogeneous. When one Zn atom is substituted by one La atom, the density of electrons surrounding La atom is higher, while the density of electrons around O atoms becomes lower. The interaction between the La atom and the surrounding ones was enhanced and a high density of overlapped charges was observed, the charges moved to lower energy levels as well (Ozgur et al., 2005; Xie et al., 2011).

Optical properties

The absorption spectra of the undoped ZnO and La-doped ZnO with different concentrations of La ions are as shown in Figure 7. In Figure 7, the absorption threshold of pure ZnO is about 3.3 eV, corresponding to the band gap of 3.37 eV. The peak value of absorption spectrum in pure ZnO located at 11 eV, which is the result of charge transfer from O-2p (-2 eV) to Zn-4s (8 eV) orbits. However, certain difference exists between peak value's location and charge transfer energy due to relaxation

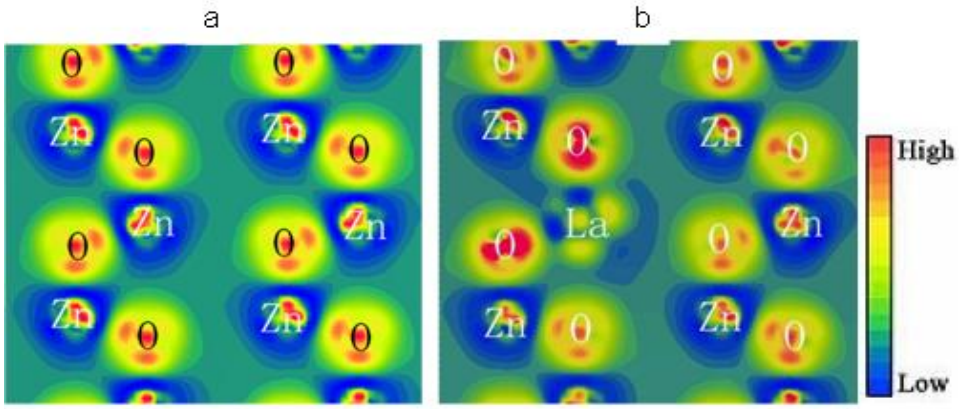

Figure 6. Plots (110) surface of difference of the charge density contour for ZnO supercells with and without La-doping. (a) M1 and (b) M3.

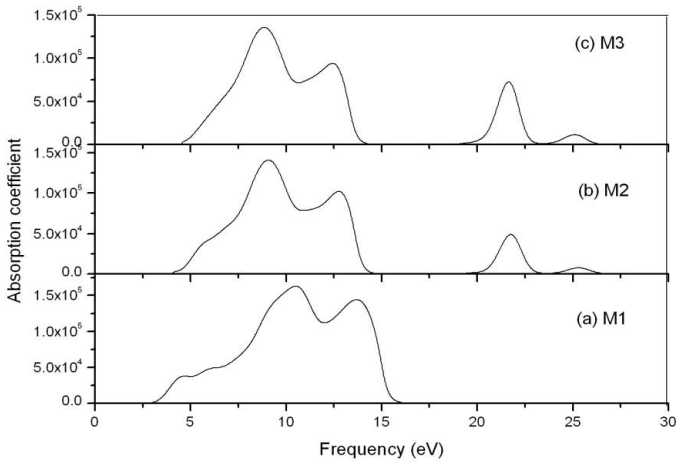

Figure 7. Calculation results of absorption spectra in the ZnO supercells. (a) without La-doping, (b) and (c) for M2 and M3, respectively.

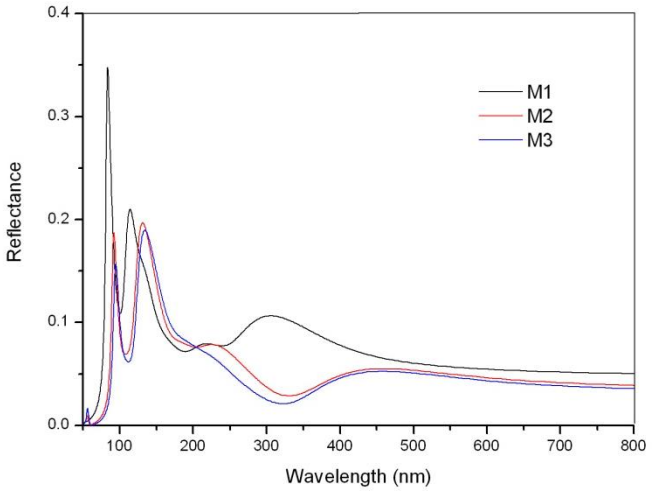

Figure 8. Calculation results of reflectance spectra for ZnO:La supercells with varying doping concentrations.

effects in electron transfer process. Compared with pure ZnO, considerable blueshift of absorption threshold in ZnO:La systems was achieved due to the wider energy gap as shown in Figures 3 and 4. In addition, the peak value of absorption coefficient decreases after La doping in ZnO systems. The optical reflectance spectra of ZnO:La system with different doping concentrations is as shown in Figure 8. All curves show relatively low reflectivity (<15%) in the visible light range. These results of calculation are consistent with experimental one pointed out in Ramakrishna et al. (2000).

Conclusions

Using a first principles plane wave pseudopotential method, the electronic structures and optical properties of La-doped ZnO system have been studied. A series of ZnO supercell models were constructed and the energy band structures, DOS and PDOS of ZnO system were calculated and analyzed. The results showed that, obvious variation and wider energy gap of energy band structures were achieved in ZnO system with La-doping. The atomic populations of the ZnO supercells showed that more than one free electron exists in La-doped ZnO supercells, and it might result in metallization of the La-doped ZnO systems. In addition, optical characteristics of ZnO system were studied. The decrease of absorption coefficient, lower reflectivity in the visible light range and the blueshift of absorption threshold were gained with the increase of La doping concentration in ZnO system. We showed good coincidence between the results of calculations an the existing experimental data, and these analyses, based on first - principles calculations

demonstrated that the La-doped ZnO was a suitable material as transparent electrodes in solar cells.

ACKNOWLEDGEMENTS

This work was supported by the National Natural Science Foundation of China (project no.61040061), Hunan Provincial Natural Science Foundation of China (project no. 11JJ2034), the City Science and Technology Project of Changsha (project no.K1106024-11) and the Fundamental Research Funds for the Central Universities of China.

REFERENCES

Anandan S, Vinu A, Sheeja LKLP, Gokulakrishnan N, Srinivasu P, Mori T, Murugesan V, Sivamurugan V, Ariga K (2007). Photocatalytic activity of La-doped ZnO for the degradation of monocrotophos in aqueous suspension. J. Mol. Catal. A-Chem., 266: 149-157.

Chowdhury R, Adhikari S, Rees P (2010). Optical properties of silicon doped ZnO. Physica. B, 405: 4763-4767.

Hoffmann MR, Martin ST, Choi WY, Bahnemann DW (1995). Applications of semiconductor photocatalysis. Chem. Rev., 95: 69-96.

Kim YI, Seshadri R (2008). Optical Properties of Cation-Substituted Zinc Oxide. Inorg. Chem., 47: 8437-8443.

Kisi EH, Elcombe MM (1989). u parameters for the wurtzite structure of ZnS and ZnO using powder neutron diffraction. Acta. Crystallogr. C, 45: 1867-1870.

Lan W, Liu Y, Zhang M, Wang B. Yan H, Wang Y (2007). Structural and optical properties of La-doped ZnO films prepared by magnetron sputtering. Mater. Lett., 61: 2262-2265.

Li P, Deng SH, Zhang L (2010). First-principle studies on the conductive behaviors of Ga, N single-doped and Ga-N codoped ZnO. Comp. Mater. Sci., 50:153-157.

Lyons JL, Janotti A, Van DVCG (2009). Role of Si and Ge as impurities in ZnO. Phys. Rev. B., 80: 205113.1-205113.5.

Ozgur U, Alivov Y, Liu C, Teke A, Reshchikov M, Dogan S, Avrutin V, Cho S, Morkoc H (2005). A comprehensive review of ZnO materials and devices. J. Appl. Phys., 98: 041301.1-041301.103.

Pauporte T, Lincot D (1999), Heteroepitaxial electrodeposition of zinc oxide films on gallium nitride. Appl. Phys. Lett., 75: 3817.

Ramakrishna KT, Gopalaswamy H, Reddy PJ, Miles RW (2000). Effect of gallium incorporation on the physical properties of ZnO films grown by spray pyrolysis. J. Cryst. Growth, 210: 516-520.

Sans J, Segura A, Manjon F, Mari B, Munoz A, Herrera-Cabrera M (2005). Optical properties of wurtzite and rock-salt ZnO under pressure. Microelectron. J., 36: 928-932.

Sehili T, Boule P, Lemaire J, (1989). Photocatalysed transformation of chloroaromatic derivatives on zinc oxide II: Dichlorobenzenes. J. Photoch. Photobio. A. 50: 103-116.

Tang X, Lu HF, Ma CY, Zhao JJ, Zhang QY (2008). Ab initio investigations on the electronic structure and optical properties of HX-ZnO. Phys. Lett., A, 372: 5372-5376.

Yu Y, Zhou J, Han H, Zhang C, Cai T, Song C, Gao T (2009). Ab initio study of structural, dielectric, and dynamical properties of zinc-blende ZnX (X = O, S, Se, Te). J. Alloy. Compd., 471: 492-497.

Vispute RD, Talyansky V, Choopun S, Sharma PP, Venkatesan T, He M, Tang X, Halpern JB, Spencer MG, Li YX, Salamanca-Riba LG (1998). Heteroepitaxy of ZnO on GaN and its implications for fabrication of hybrid optoelectronic devices. Appl. Phys. Lett., 73: 348-350.

Wan QX, Xiong ZH, Dai JN, Rao JP, Jiang FY (2008). First-principles study of Ag-based p-type doping difficulty in ZnO. Opt. Mater., 30: 817-821.

Xie HQ, Chen Y, Huang WQ, Huang GF,P Peng, Peng L, Wang TH, Zeng Y (2011). Optical Characteristics of La-Doped ZnS Thin Films Prepared by Chemical Bath Deposition. Chin. Phys. Lett., 28: 027806.

Xie HQ, Zeng Y, Huang WQ, Peng L, Peng P, Wang TH (2010). First-principles study on electronic and optical properties of La-doped ZnS. Int. J. Phys. Sci., 5: 2672-2678.

Xie HQ, Zeng Y, Zeng JP (2011).Analysis and simulation of lateral PIN photodiode gated by transparent electrode fabricated on fully-depleted SOI film. J. Cent. South. Univ. T, 18(3): 744-748.